

VORTEX FORMATION IN THE WAKE OF AN OSCILLATING CYLINDER

C. H. K. WILLIAMSON AND A. ROSHKO

*Graduate Aeronautical Laboratories, California Institute of Technology, Pasadena,
California 91125, U.S.A.*

(Received 4 August 1987 and in revised form 14 January 1988)

When a body oscillates laterally (cross-flow) in a free stream, it can synchronize the vortex formation frequency with the body motion frequency. This fundamental “lock-in” regions is but one in a whole series of synchronization regions, which have been found in the present paper, in an amplitude-wavelength plane (defining the body trajectory) up to amplitudes of five diameters. In the fundamental region, it is shown that the acceleration of the cylinder each half cycle induces the roll-up of the two shear layers close to the body, and thereby the formation of four regions of vorticity each cycle. Below a critical wavelength, each half cycle sees the coalescence of a pair of like-sign vortices and the development of a Karman-type wake. However, beyond this wavelength the like-sign vortices convect away from each other, and each of them pairs with an opposite-sign vortex. The resulting wake comprises a system of vortex pairs which can convect away from the wake centerline. The process of pairing causes the transition between these modes to be sudden, and this explains the sharp change in the character of the cylinder forces observed by Bishop and Hassan, and also the jump in the phase of the lift force relative to body displacement. At precisely the critical wavelength, only two regions of vorticity are formed, and the resulting shed vorticity is more concentrated than at other wavelengths. We interpret this particular case as a condition of “resonant synchronization”, and it corresponds with the peak in the body forces observed in Bishop and Hassan’s work.

1. INTRODUCTION

THE PROBLEM of a cylindrical body oscillating laterally in a free stream has received a great deal of attention owing mainly to its practical significance (see for example the reviews of Bearman [1] and of Sarpkaya [2]). If a cylinder is placed in a flow, it experiences a fluctuating lift force (transverse to the flow) caused by the asymmetric formation of vortices, which can cause a structure to vibrate. One of the fundamental features of flow-induced vibration is the ability of the structure oscillating at its natural frequency (f_n) to synchronize the vortex shedding frequency. The range of frequency ratios (f_n/f_s)† over which this “lock-in” of frequencies is possible increases as the oscillation amplitude increases. Wakes of oscillating bodies are also of relevance to the case of a fixed body placed under waves and in currents, where the relative oscillatory fluid motion can be of much larger amplitude than is normally studied in other vibration problems. In the present experiments, by forcing a cylinder to oscillate up to large amplitudes in a free stream, we can investigate under more controlled conditions how a body influences its own wake to cause synchronization.

In the case of a cylinder oscillating transversely in a free stream, the relevant parameters, besides Reynolds numbers, are the dimensionless oscillating amplitude (A)

† f_s = vortex shedding frequency of a non-oscillating cylinder.

and frequency f_e (or period T_e). However, instead of the latter we prefer to use the wavelength (λ) of the corresponding sine wave trajectory along which the body travels relative to the fluid. This, in fact, is the natural point of view in the frame of reference of a towing tank, which is the facility used for the present experiments. Thus the relevant parameters are

$$\text{Reynolds number, } \text{Re} = \frac{UD}{\nu},$$

$$\text{Amplitude ratio} = A/D,$$

$$\text{Wavelength ratio} = \frac{UT_e}{D} = \frac{\lambda}{D},$$

where U is the velocity in the x -direction, and T_e is the period of cylinder oscillation in the transverse y -direction. (The normalized wavelength is equivalent to what is usually referred to as the reduced velocity.) Emphasizing the *trajectory* in the point of view is often useful to better understand the cylinder-vortex interaction, as well as effects of cylinder accelerations on the vortex formation.

Important features of how the forces on the body are influenced by forcing a cylinder to oscillate were highlighted by Bishop and Hassan [3]. They found that the forces reached a peak or "resonance" at an excitation frequency slightly below the natural shedding frequency, rather like the response of a simple oscillator to harmonic forcing. At a point when the lift force drops sharply (as trajectory wavelength is increased), the phase (ϕ) between the lift and the body motion also changes abruptly, as shown in Figure 1(a) and (b). The system is also hysteretic in that the precise position of the phase "jump" depends on whether the wavelength is increased or decreased, (i.e. on the history of the motion). Feng [4] observed a similar phase jump for an unforced elastically-mounted cylinder at a point where the response amplitude and lift change abruptly, and again found hysteresis in some of his experiments; an example is shown

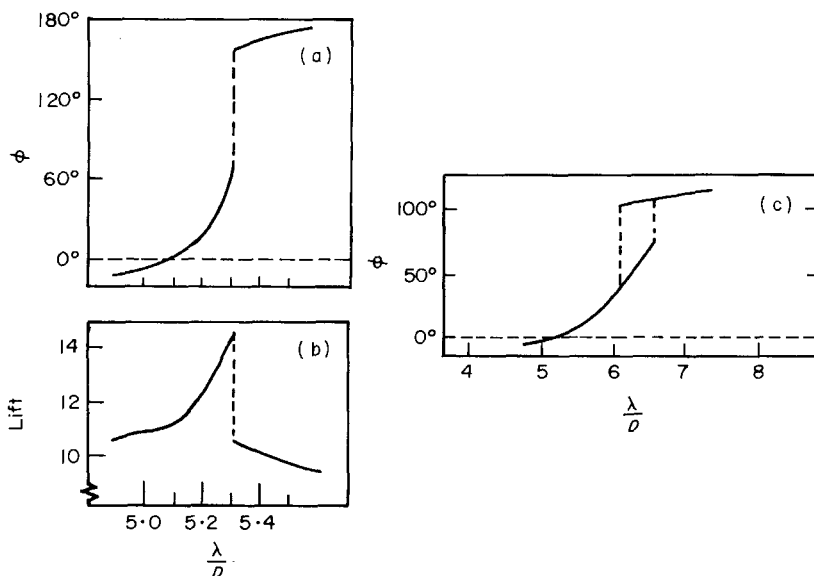


Figure 1. Variation of lift force and its phase (ϕ) as wavelength (λ) is varied. (a) and (b) are for a cylinder forced to oscillate, from Bishop and Hassan [3]. (c) is for an elastically-mounted cylinder from Feng [4].

in Figure 1(c). The importance of the phase in these problems lies in the fact that it strongly influences the energy transfer from the fluid to the body motions. Although several authors have had some success in modelling the nonlinear vibration response of an elastically-mounted cylinder with differential equations (e.g., Hartlen, Baines and Currie [5], Berger [6]), a complete understanding of the character of the forces and responses should include a knowledge of the vortex dynamics which cause the phenomena.

Recent work by Zdravkovich [7] who examined other published visualization results [8–11], and by Öngören and Rockwell [12] demonstrate that there is a change in the timing of the vortex shedding on either side of the phase jump. Zdravkovich deduced that, at shorter trajectory wavelengths, a vortex forming on one side of a cylinder was shed when the cylinder was near the maximum displacement on the opposite side, but the converse seemed to occur at longer wavelengths. Öngören and Rockwell observed a similar result, and also concluded that the “swinging” of the near wake, which increased suddenly after a critical wavelength, was likely to be “intertwined” with the peak in the lift force. A particularly interesting result, from their velocity measurements, is that the phase jump occurs for circular and triangular sections but not for a square section, demonstrating the importance of afterbody shape.

If the phase of the lift force changes sharply, it seems evident that there must be an abrupt change in the timing and possibly the character of the vortex formation. That is, the force on the body can be decomposed into a potential or added mass term, plus a vortex force term which results from the rate at which the impulse of the shed vorticity (including its image vorticity) is changing (see, for example, Lighthill [13] for a discussion of this decomposition). The potential term changes continuously if the wavelength of the body's trajectory or the oscillation period is gradually increased, so we expect that an abrupt change in the cylinder force can only be due to an abrupt change in the vortex force, i.e., to a sharp change in the dynamics of the shed vorticity. A central question which is addressed in the present paper is: Why does the vortex formation change its character through synchronization, and why does it change so suddenly at a critical wavelength?

The synchronization that is discussed above occurs in a region in the (λ, A) plane marked B in Figure 2, where there have been a large number of papers studying this *fundamental synchronization*. There has also been some investigation in the regions marked C within which superharmonic or subharmonic vortex shedding modes have been found (for example, Öngören and Rockwell [12] and Stansby [14]). Another region (or line) in the (λ, A) plane which has previously received attention is the A/D axis, marked A, which is the case of “planar oscillatory flow,” (i.e., zero free-stream velocity). In this case, repeatable vortex patterns involving 1, 2 and 3 vortices shed per half cycle have been found for certain ranges of amplitude (marked 1, 2, 3, respectively, in Figure 2 and taken from Williamson [15]). The above regions constitute the main areas in the (λ, A) plane which have been studied before. One of the major questions in the present paper is: what other regions of vortex synchronization exist in the (λ, A) plane? Also, what happens to the vortex formation in the region of the fundamental synchronization (region B) as the amplitude is gradually increased beyond the shaded region in Figure 2?

Due to the transverse oscillations, the cylinder is continually accelerating and decelerating along its trajectory through the fluid. In the fundamental synchronization region, we find that the vortex dynamics close behind the body are affected by this changing acceleration, and we observe a sharp changeover from one mode to a markedly different mode of vortex formation across a critical boundary in the

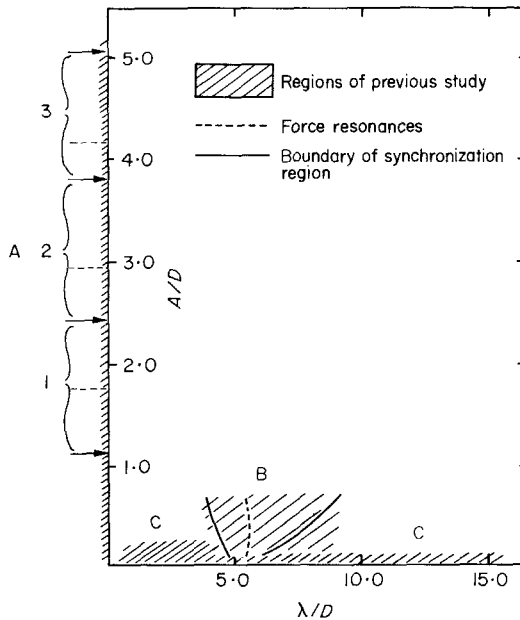


Figure 2. Schematic diagram showing the main regions of previous studies in the wavelength–amplitude ($\lambda/D, A/D$) plane.

wavelength-amplitude plane. The vortices in the wake are not simply the result of one vortex shedding each half cycle, as usually assumed (see for example the reviews in References [1] or [2]), but rather the wake involves the roll up of four separate vortices each cycle. Below the critical trajectory size, a pair of like-sign vortices amalgamate in each half cycle, whereas above the critical condition the four vortices from each cycle organize themselves into two vortex pairs convecting away from the wake centerline. The above observations, which have been briefly reported elsewhere [16, 17], are described and explained in some detail in Section 4. In Section 3 an outline is given of several other different synchronization patterns that have been found, by extending the range of amplitudes and wavelength investigated, and these are described with reference to the (λ, A) plane.

2. EXPERIMENTAL METHODS

The present paper reports on the first piece of research carried out in a new X-Y towing tank, recently installed in our laboratory. The tank, which was designed with flow visualization in mind, has glass panels around all sides and the bottom. They are housed in a steel framework, with the side glass plates running the whole 15 ft (4.57 m) length of the $3\frac{1}{2}$ ft (1.07 m) deep by $3\frac{1}{2}$ ft wide tank. The two-way (X-Y) carriage system rides over the top of the tank using wheels on linear shafts, and operates much like a computer X-Y plotter.

The flow visualization method uses aluminium particles on the fluid surface, and this technique has been used in conjunction with a dye method beneath the surface to show that the vortex patterns are similar. However, in the present work only the surface technique is included, while the results of the dye technique will be reported later.

In Section 3, we will discuss a “map” of different vortex synchronization patterns in the (λ, A) plane. This map of lock-in regions was derived painstakingly from tests at

A/D intervals of 0.25 and λ/D intervals of 1.0 over much of the (λ, A) plane, although near the fundamental lock-in region ($0.2 < A/D < 1.8$; $1.0 < \lambda/D < 10.0$) repeated tests were conducted with a finer resolution of (λ, A) points: A/D intervals of 0.1 and λ/D intervals of 0.5.

3. OUTLINE OF VORTEX SYNCHRONIZATION REGIONS IN THE (λ, A) PLANE

The main thrust of previous research with oscillating bodies has been in the fundamental lock-in region near the area marked "2S" in the map of regions in the (λ, A) plane shown in Figure 3(a), and also in the other regions that were discussed in the Introduction, with reference to Figure 2. One of the purposes of the present research was to study the types of wake synchronization that may occur throughout a much larger region in the (λ, A) plane than has been studied before.

In the case of planar oscillatory flow past a body, Bearman *et al.* [18] and Williamson [15] found repeatable vortex shedding patterns, each one occurring within a certain range of amplitudes. The process of pairing of vortices was found to be fundamental not only for repeatability of the patterns but also for enabling vortices to convect away (from the local body region) under their own induced velocities. In several of the present vortex patterns, vortex pairing is again a fundamental feature of the wake dynamics, as can be seen diagrammatically in the types of patterns shown in Figure 3(b). The diagrams of patterns in Figure 3(b) refer to the wakes found in regions of the (λ, A) plane in 3(a), and have been designated by combinations of P meaning vortex Pair, and S meaning a Single vortex; e.g., P + S means a pattern where in each cycle a vortex pair and a single vortex are shed. In Figure 3(b) the dashed lines enclose those vortices formed in one complete cycle.

In Figure 3(a) the horizontal T_e/T_s axis[†] is also drawn (approximately) for reference; the value used for T_s is that derived assuming that the Strouhal number $S = D/UT_s$ is equal to 0.20 for all the Reynolds numbers investigated. The parameter (T_e/T_s) is related to λ/D by the expression $(T_e/T_s) = S(\lambda/D)$, so near the fundamental lock-in $T_e \approx T_s$, and therefore $\lambda/D \approx 5.0$, i.e. the cylinder travels roughly five diameters in each cycle of shedding (and sheds two vortices, one of each sign).

The major vortex patterns near the fundamental lock-in region are 2S, 2P and P + S. The designation 2S means that in each half cycle a vortex is fed into the downstream wake, like the natural Karman vortex shedding; 2P means the formation of vortex pairs which convect laterally outwards from the wake centerline, and the P + S mode is an asymmetric version of the 2P mode where the cylinder sheds a pair and a single vortex each cycle [see the sketches in Figure 3(b)]. Other patterns are denoted C(2S) and C(P + S) which means that near the cylinder we have the 2S or P + S modes but the smaller vortices coalesce either immediately behind the body or within about 15 diameters, into larger scale structures (the sketch shows an extreme example of this).

The regions marked P and 2P* refer to vortex patterns similar to those referred to as "single pair" and "double pair" by Williamson [15]. Mode P is a wake made up of a set of vortex pairs convecting downstream but out to one side (the side depends on the history of the flow) and takes on the appearance of a jet rather than a wake. Mode 2P* is similar to 2P except that vortex pairs in one of the half cycles convect away from in front of the body. In this case, the convection of each pair is in the downstream direction (creating a jet), rather than in the upstream direction for the 2P mode. The

[†] T_s = period of vortex shedding for a non-oscillating cylinder.

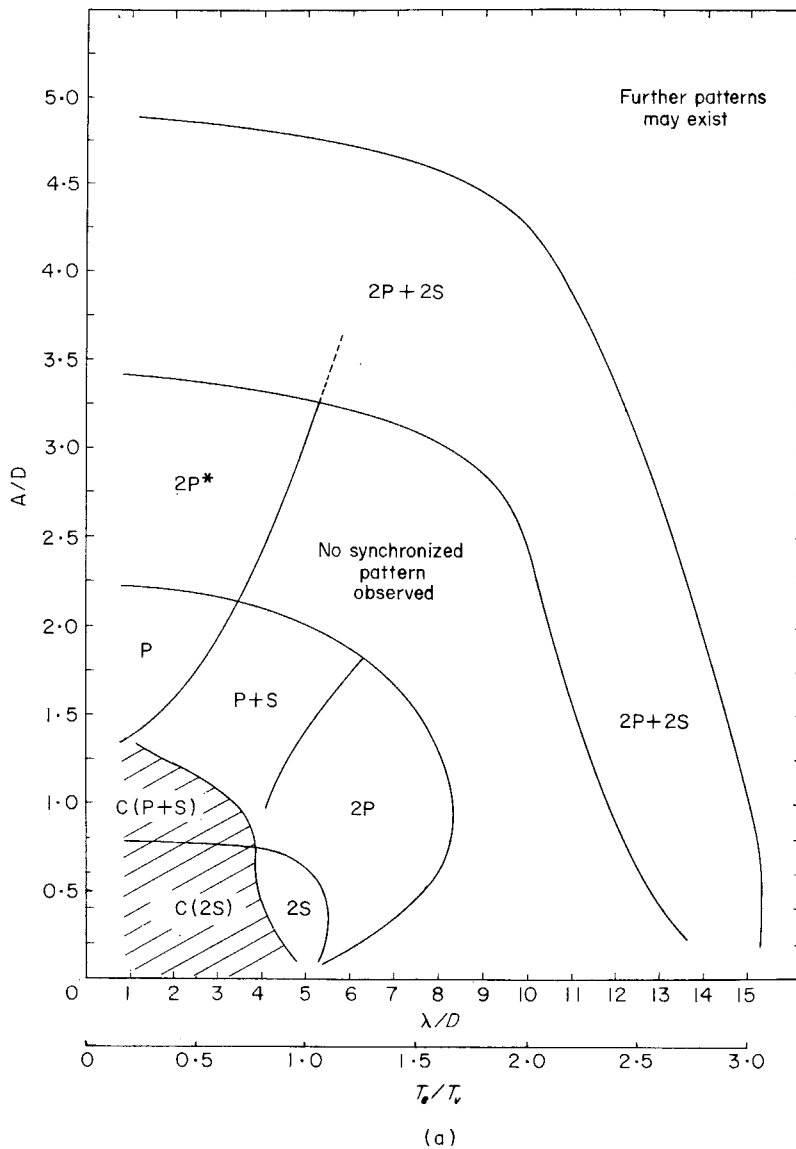


Figure 3(a). Map of vortex synchronization regions in the wavelength-amplitude (λ/D , A/D) plane, as found in the present study.

present experiments were conducted for a range of λ/D down to 1.0, and the boundaries between the P, $2P^*$ and $2P+2S$ modes in Figure 3(a) only roughly correspond with those for $\lambda/D = 0$ (from Reference [15]) which are shown schematically in Figure 2. The way in which the regions for $\lambda/D > 0$ are connected with those found previously for $\lambda/D = 0$ was not studied in detail here and there may be some interesting changes in the process of vortex formation as $\lambda/D \rightarrow 0$, especially in the region for $A/D < 1.2$. For example, the coalescence of small-scale vortices into a large-scale street-type wake for $\lambda/D > 0$ found here, changes to a different mode when $\lambda/D = 0$, which is described in Reference [15] as the "pairing of attached vortices".

Finally, a vortex pattern called $2P + 2S$ comprises two vortex pairs forming at the top

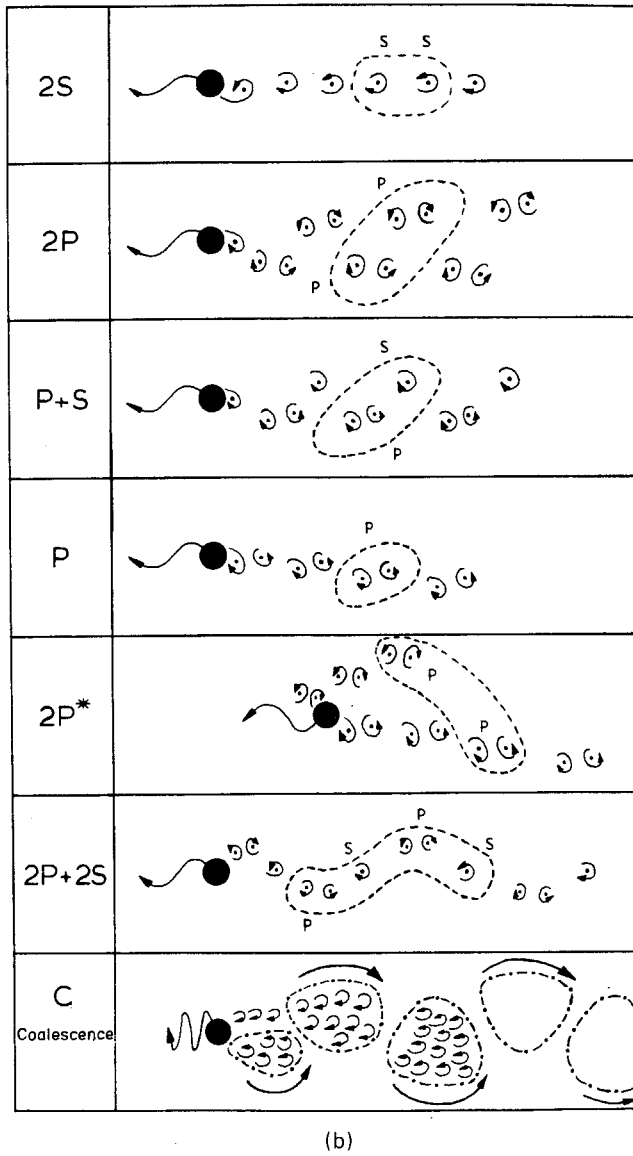


Figure 3(b). Sketches of the vortex shedding patterns that are found in the map in (a). "P" means a vortex pair and "S" means a single vortex, and each pattern is defined by the number of pairs and single vortices formed per cycle; ----- encircles the vortices shed in one complete cycle.

and bottom of the body trajectory as in the 2P mode, but with the inclusion of single vortices between each vortex pair [see the sketch in Figure 3(b)]. The fact that the 2P + 2S mode exists near $T_e/T_s \approx 3$ (i.e. a $\frac{1}{3}$ -subharmonic), without a similar mode occurring near $T_e/T_s \approx 2$ (a $\frac{1}{2}$ -subharmonic), will be discussed in Section 5. The "empty" region in the (λ, A) plane between the region for 2P and 2P + 2S represents those conditions where no periodic synchronized mode of vortex formation was observed in the present study.

The boundaries between regions in Figure 3 can only be regarded as approximate, although much care was taken to construct what is called the "critical curve" in Figure 4, and other boundaries nearby. This figure shows the fundamental lock-in region in

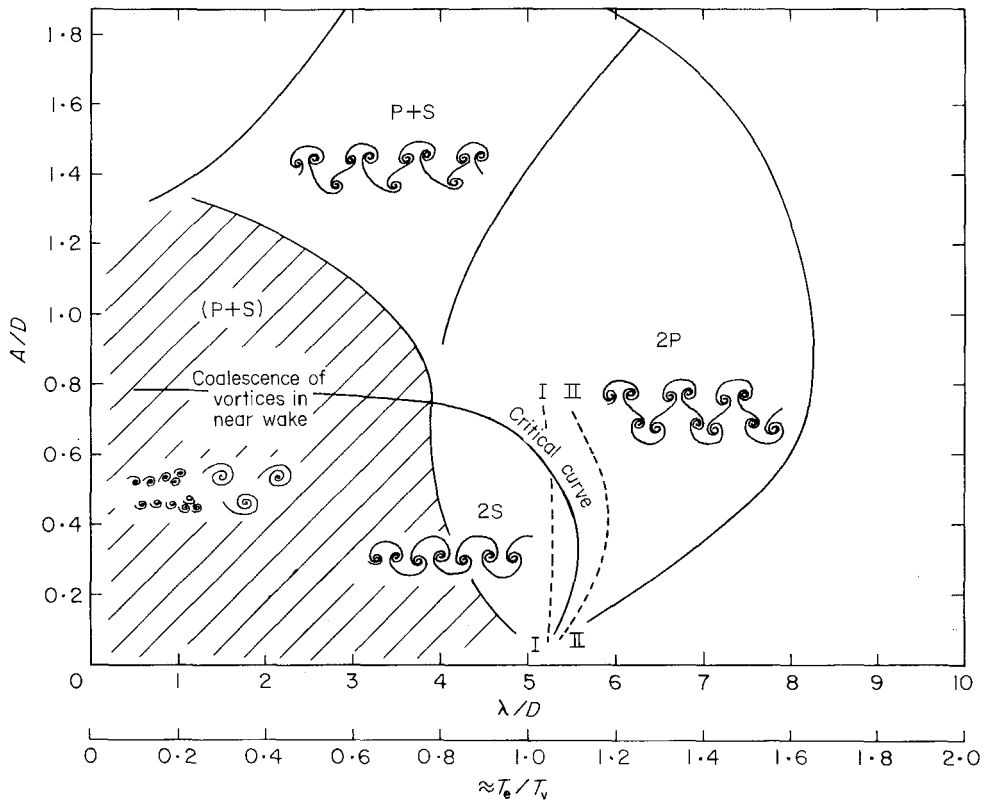


Figure 4. Map of vortex synchronization patterns near the fundamental lock-in region. The critical curve marks the transition from one mode of vortex formation to another. I, II are the curves where the forces on the body show a sharp "jump"; from Bishop and Hassan [3]. I is for wavelength decreasing and II is for wavelength increasing.

detail. It can be seen that the curves do not reach the λ axis, as there is a threshold amplitude necessary before lock-in occurs, although its precise value was not determined here. (Koopmann [19] reports lock-in for $A/D > 0.05$). The boundary between the P + S and 2P modes as shown is roughly correct for $300 < Re < 1000$, but for $Re < 300$ the P + S mode occurred instead of the 2P mode throughout that region as well. The reason why the P + S mode takes the place of the 2P mode at low Re has not yet been determined.

The relevant parameters in the present problem are, as defined earlier, the amplitude ratio, the wavelength ratio and the Reynolds number (Re) based on the streamwise-velocity, U . Ideally one would want to explore the parameter space (λ, A) while keeping the Reynolds number fixed, and repeat the experiments for a number of different Re . However, in the present series of experiments, it was found more practical to keep Re within a certain range, $300 < Re < 1000$. For a non-oscillating body, in this range of Re , the Strouhal number[†] for the vortex shedding remains nearly constant, as it does up to Reynolds numbers of around 10,000. If we make the assertion that the dynamics of the vortices in the near wake is basically inviscid over this range of Re , then we can expect the process of vortex formation (for the present

[†] Strouhal number, $S = f_s D / U$.

case of the oscillating body) to be similar at each particular value of (λ, A) over the range of Re used here. We assume that our map of vortex patterns in Figure 3 is representative of those patterns to be found over a large range of Re . However, we intend to carry out further work to confirm this, and determine how these patterns and their boundaries are affected by a variation of Reynolds numbers.

Wake patterns similar to the P + S and 2P modes have been found recently in a number of different flows, but all of them involved an oscillating body or an oscillating component in the flow around the body. Koochesfahani [20] observed the P + S and 2P modes for a pitching airfoil, but found the P + S to occur only when the oscillation waveform was non-symmetric. Griffin and Ramberg [21] and Öngören and Rockwell [22] observed the two modes when a cylinder vibrated in-line with a flow at a period roughly half the natural shedding period, but Öngören and Rockwell did not find similar modes when the oscillation was transverse to the flow, as we have found here. Couder and Basdevant [23] found the 2P and P + S modes for a cylinder travelling with in-line oscillations in a soap film, and very recently DeTemple [24] has shown the 2P and P + S modes to occur when the flow about a cylinder is subjected to small oscillations, generated by sound, that are parallel to the free stream. Finally, both Honji and Taneda [25] and Griffin and Ramberg [11] found that the shedding of a third vortex per cycle, which corresponds with the P + S mode, could occur at large amplitudes. In the above studies it was not known over what range of (λ, A) -parameters these modes occurred, nor has the relation between the shedding patterns and the forces on the bluff bodies been investigated. The first question has been considered in the present section, and in the following Section 4 we consider the relation between the forces and the shedding patterns. The jump in the lift characteristics is explained by a jump in vortex mode which itself is brought about by the fact that the body is continually accelerating/decelerating. We will see that this jump across the critical curve is actually a sharp transition from the 2S to the 2P mode of vortex formation.

4. VORTEX FORMATION IN THE FUNDAMENTAL SYNCHRONIZATION REGION

In this Section, results are shown of flow observations in the neighborhood of the fundamental lock-in region discussed in Section 3. The curves (marked I and II in Figure 4) at which Bishop and Hassan discovered a sharp change in the character of the body forces, is associated in the present paper with an abrupt transition from one state of vortex formation (2S) to another state (2P). In both modes the vortex formation is subtly different from the case of single vortices forming and shedding each half cycle, as was previously thought to occur. The fact that the body accelerates in the first half of each half cycle causes the roll-up of four regions of vorticity per cycle, as will be discussed in Section 4.1. Below a critical trajectory size, two like-signed vortices amalgamate in each half cycle to create a vortex street-type wake or 2S mode. Above this critical size, vortex amalgamation does not occur, and the four regions of vorticity arrange themselves in the form of two vortex pairs, i.e., the 2P mode appears.

An immediate view of how the vortex formation changes as the trajectory wavelength λ is increased can be seen at a small amplitude of $A/D = 0.3$ in Figure 5, with the camera fixed with respect to the undisturbed fluid. The values of λ/D are such that in (b) and (c) the vortex formation is periodic and synchronized in the 2S and 2P modes respectively. In (a) the value of λ/D is just below that for which the 2S synchronization occurs, although the appearance and general configuration of the

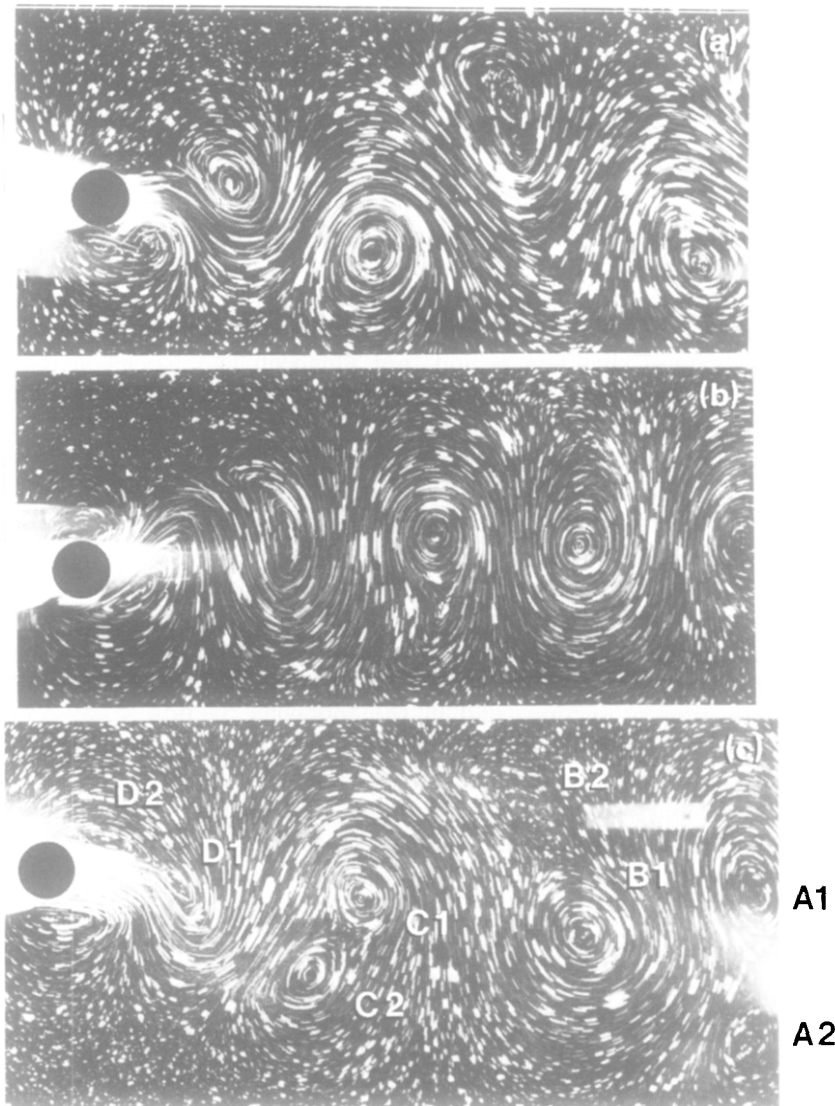


Figure 5. Wakes of an oscillating cylinder for three different wavelengths, at an amplitude of 0.3 diameters and for Reynolds number = 392. (a) $\lambda/D = 3.75$ ($T_e/T_v = 0.77$); (b) $\lambda/D = 5.0$, ($T_e/T_v = 1.03$); (c) $\lambda/D = 6.5$, ($T_e/T_v = 1.33$). Visualization is fixed with respect to the undisturbed fluid.

near-wake vortices for low values of λ/D within the 2S region remains very similar to (a). There are two clear effects to the vortex street-type of wake (2S mode) which occur as the wavelength λ is increased, and which may be observed by comparing (a) and (b). With an increase in imposed wavelength λ , the lateral distance between wake vortices decreases, and also the wake wavelength (or longitudinal distance between the vortices) increases. However, the change in the vortex formation between (b) and (c) is more dramatic; there is a mode change between (b) for which the imposed wavelength is "pre-critical", and (c) for which the wavelength is "post-critical". For example, the anticlockwise vortices A_1 and A_2 in (c) were shed in one half cycle, followed in the next half cycle by clockwise vortices B_1 and B_2 , then anticlockwise vortices C_1 and C_2 , and finally in the present half cycle clockwise vortices D_1 and D_2 are shedding. (The

terminology "pre-critical" and "post-critical", which is found to be useful in the present context, should not be confused with other uses of these terms such as, for example, precritical and postcritical Reynolds numbers used for very much higher velocities, where the boundary layer on the body becomes turbulent). These pairs of vortices in the 2P mode are evident in (c), although the process of pairing is made more obvious later in Figure 13.

4.1. THE VORTEX DYNAMICS THAT CAUSE A MODE CHANGE

Why does the wake change in character through the lock-in region? In order to answer this question, the flow is visualized at a slightly larger amplitude and from a reference frame fixed with respect to the cylinder, in Figures 6–8. The amplitudes are $A/D = 0.4$

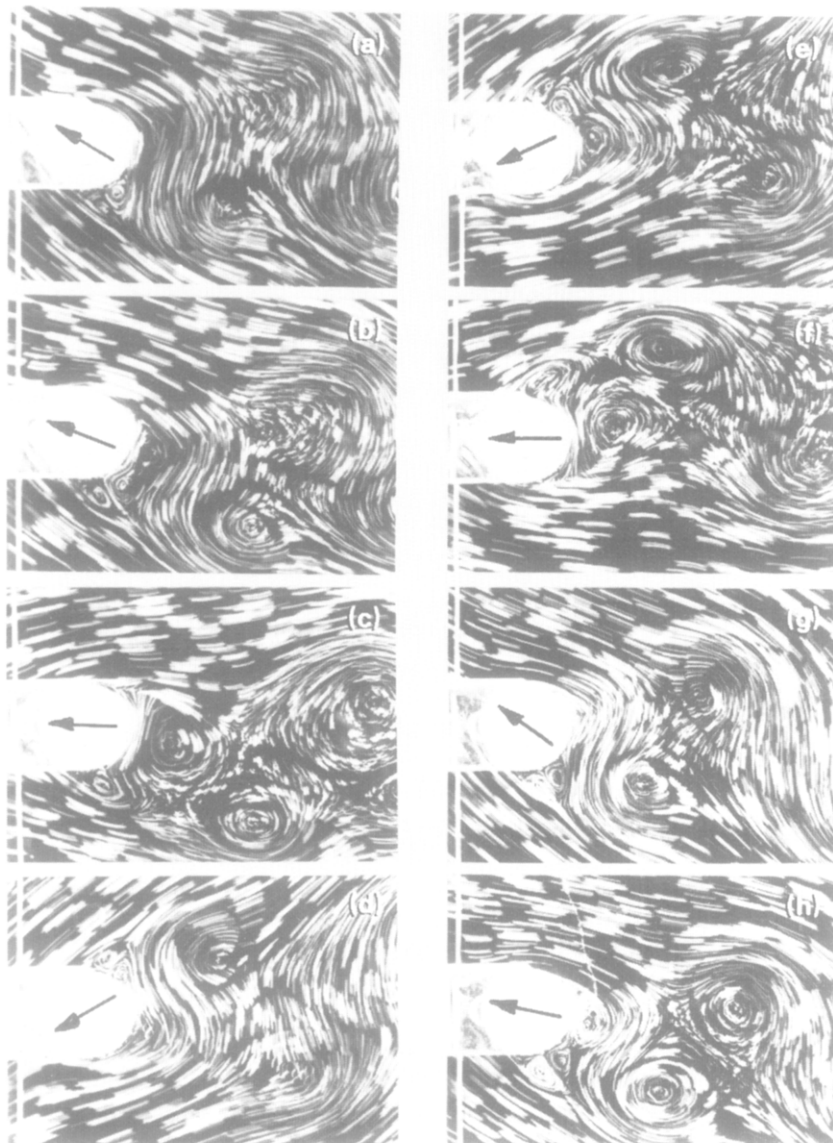


Figure 6. "2S" mode of formation at the low-wavelength end of the fundamental lock-in region. $\lambda/D = 4.5$, $A/D = 0.5$, $Re = 392$ ($T_e/T_v = 0.93$). Visualization fixed with respect to the cylinder.

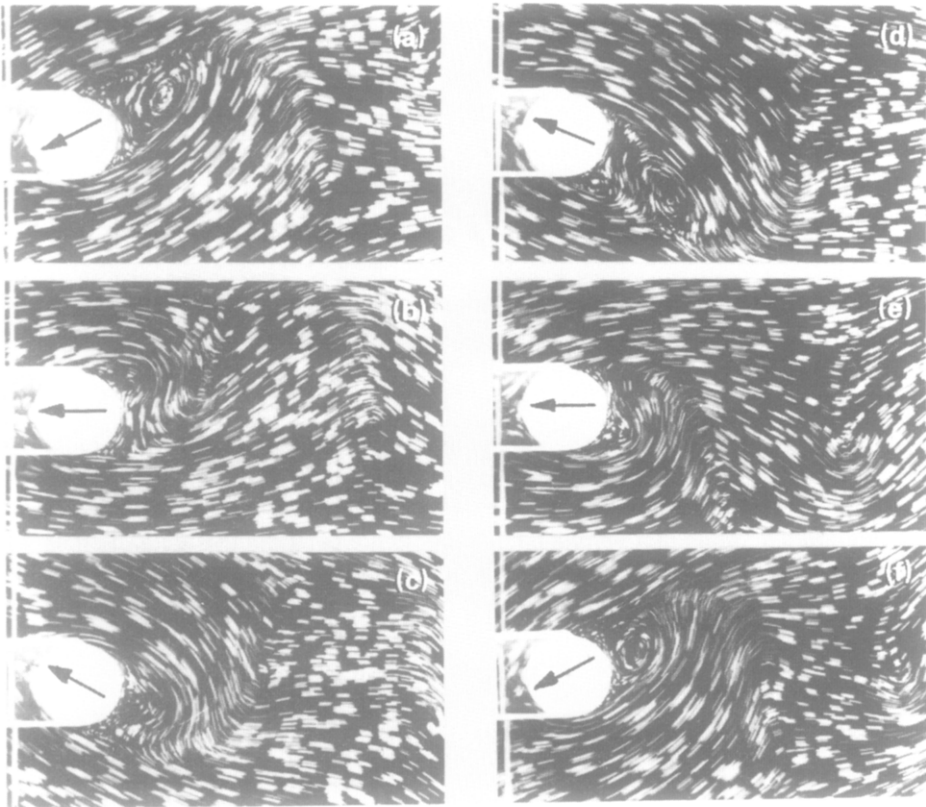


Figure 7. "2S" mode of formation at just-precritical wavelength. $\lambda/D = 5.0$, $A/D = 0.4$, $Re = 392$, ($T_e/T_v = 1.03$). Visualization fixed with respect to the cylinder.

or 0.5, and the wavelengths are $\lambda/D = 4.5$ (low λ but synchronized), $\lambda/D = 5.0$ (just pre-critical) and $\lambda/D = 5.5$ (post-critical). To understand these figures, schematic diagrams have been drawn by tracing the vortex positions onto correctly-scaled computer plots of the cylinder path, in Figures 9–11. What can be seen at a glance in Figures 9 and 11 is the fact that four vortices are formed each cycle, rather than two as has been assumed in other studies. This feature is fundamental to the mode jump shown below.

The key to understanding the flow comes from noting how the dynamics of a certain vortex is affected by an increase in the wavelength of the body trajectory. We look, in turn, at the vortices marked E_1 , D and D_1 in Figures 9, 10 and 11, respectively, as these are all vortices that begin their growth in one half cycle, and shed in the next half cycle. [Note the present definition of a half cycle as shown in Figure 9(a)]. They are the equivalent vortices in each of the figures with which we can make a comparison, and thereby demonstrate the essential changes in wake formation as the wavelength is increased.

At low $\lambda/D = 4.5$ ($T_e/T_s = 0.93$) in Figure 9, we follow the motion of vortex E_1 , which rolls up in the wake as the cylinder moves upwards in (a), and subsequently is convected round the cylinder anti-clockwise in (b) and (c). As the cylinder accelerates down between (c) and (d) a pair of vortices F_1 and E_2 are formed whilst E_1 is still convecting round the body. When the cylinder reaches the bottom of the trajectory in

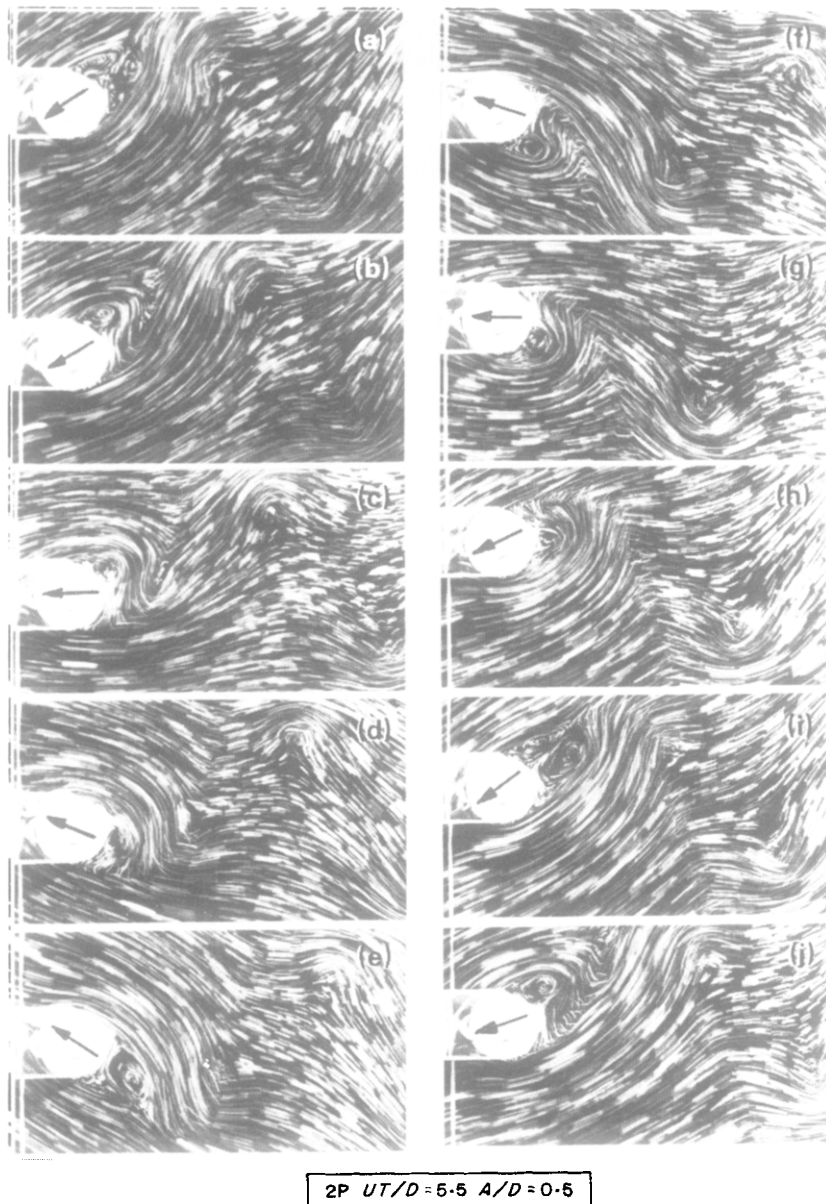


Figure 8. "2P" mode of formation at postcritical wavelength. $\lambda/D = 5.5$, $A/D = 0.5$, $Re = 392$ ($T_e/T_v = 1.13$). Visualization fixed with respect to the cylinder.

(e) and (f), vortex E_1 convects vortex E_2 of the same sign between itself and the body, and their merger causes one region of vorticity to shed in (f). Then vortex F_1 follows a history similar to that of E_1 , and so on. The downstream wake is therefore of the 2S mode with each region of vorticity the result of two like-signed vortices amalgamating. The merged vortex $E_1 + E_2$ (or simply E) in (f) is shed, roughly, when the cylinder reaches the end of a half cycle (defined as in (a)), which explains the wide lateral spacing between vortices in the street wake. This in turn leads to a larger upstream

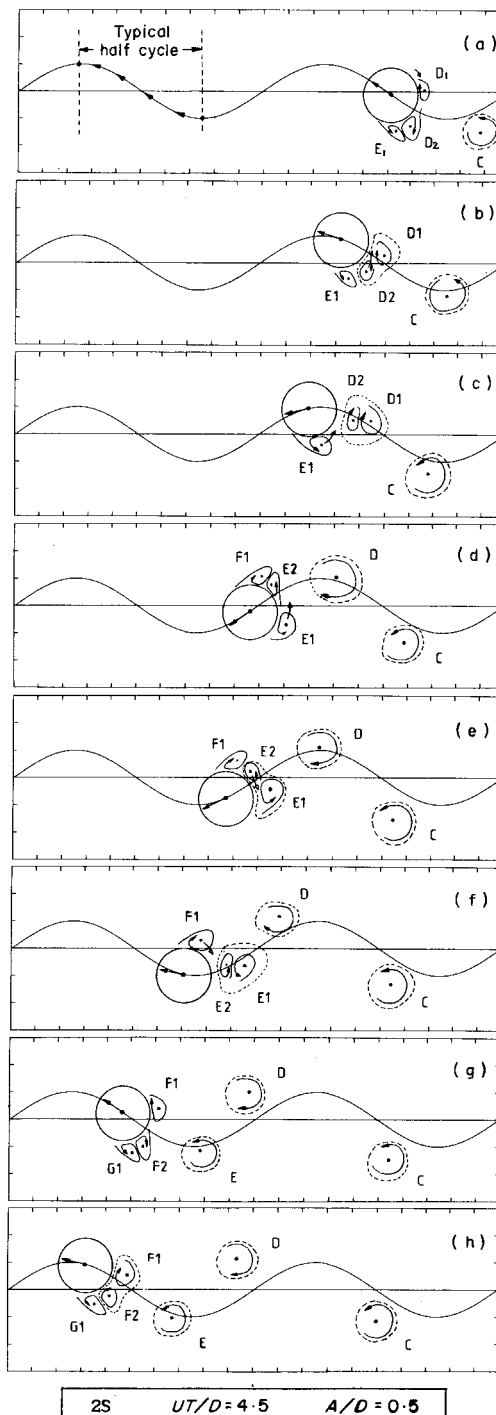


Figure 9. "2S" mode. Sketch of vortex motions taken from Figure 6. $\lambda/D = 4.5$, $A/D = 0.5$, $Re = 392$

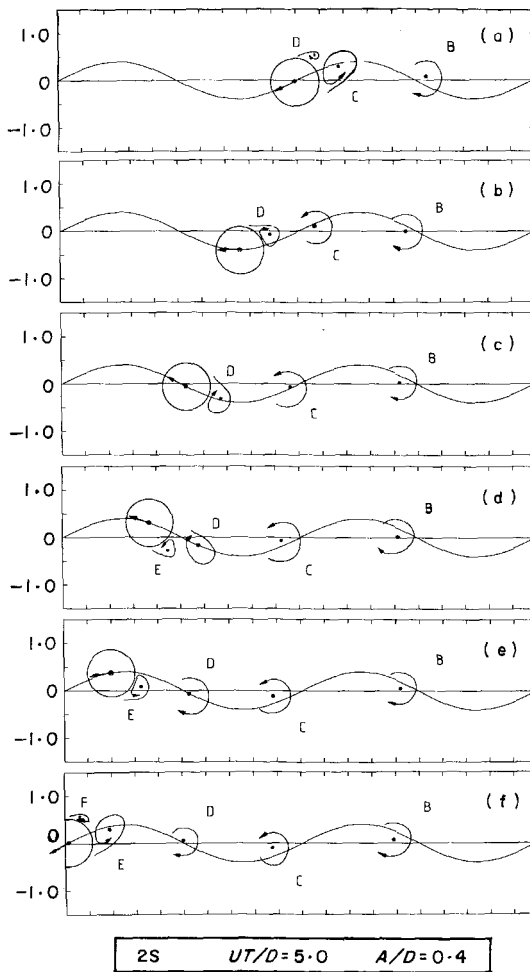


Figure 10. "2S" mode. Sketch of vortex motions taken from Figure 7. $\lambda/D = 5.0$, $A/D = 0.4$, $Re = 392$.

vortex street velocity than would be found for smaller lateral spacing† (at larger λ) and is consistent with the experiments of Koopmann [19].

To see how the history of such a vortex as E_1 is affected by an increase in trajectory wavelength, we now look at the dynamics of an equivalent vortex D at a larger wavelength in Figure 10, where $\lambda/D = 5.0$ ($T_e/T_s = 1.03$). Vortex D forms when the cylinder moves downwards in (a), and convects around the body clockwise in (b), but because the trajectory is longer than before it reaches the rear of the body earlier (than did E_1), in this case during the phase at which the body accelerates upwards. The clockwise shear layer is rolled up into D during this phase, and the anticlockwise shear layer starts to roll up into E. Vortex D sheds, roughly, when the body reaches the wake centerline in (c). The lateral vortex spacing is thereby reduced, and the upstream vortex street velocity is also reduced. This is again consistent with Koopmann's observations. The strength of vortex D will have some effect on its convection velocity

† The increased upstream velocity may be illustrated by the velocity formula for a point vortex street configuration, given by $U_v = \Gamma(\tanh \pi b/a)/2a$, where b = lateral vortex spacing, a = longitudinal spacing and Γ = vortex strength.

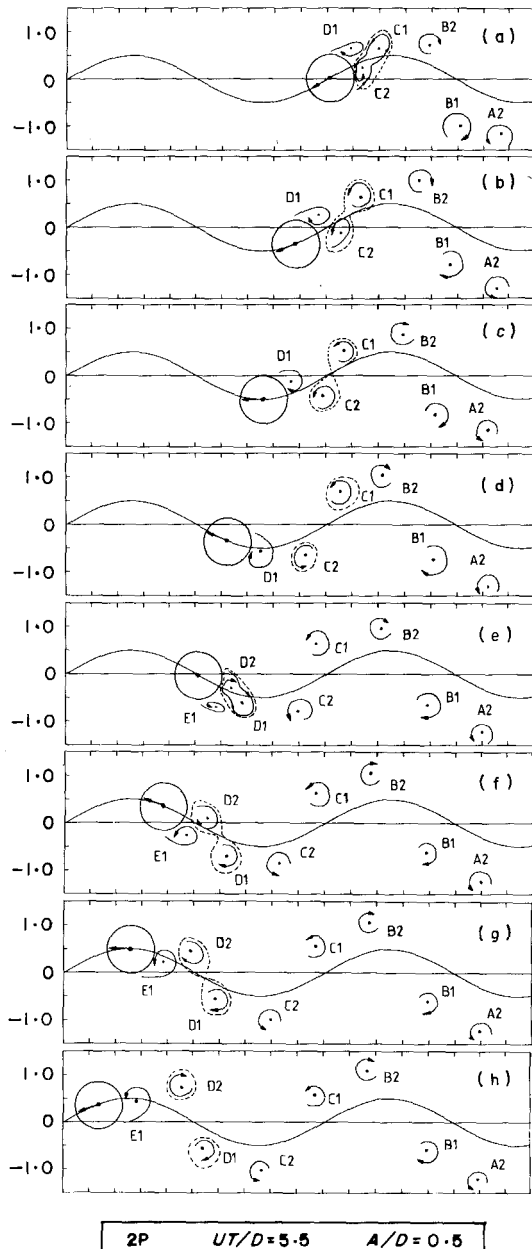


Figure 11. "2P" mode. Sketch of vortex motions taken from Figure 8. $\lambda/D = 5.5$, $A/D = 0.5$, $Re = 392$.

around the cylinder because of the induced velocity from its image in the body, although this aspect is not studied in detail in the present work.

With an increase in trajectory wavelength in Figure 11 ($\lambda/D = 5.5$, $T_e/T_s = 1.13$) the motion of our equivalent vortex is now distinctly different. The vortex to observe is D_1 , which, like E_1 and D in the previous figures, forms during one half cycle to shed in the next. The vortex D_1 reaches the rear of the cylinder earlier during the cycle than did E_1 or D , for two main reasons. First, it effectively has more time because the trajectory is longer, and secondly, its convection round the cylinder is speeded up by the effect of

C_2 , as seen in (b), (c), (d). It now sheds early in the upward-moving half cycle in (d), (e), and the acceleration upwards causes a pair of trailing vortices, D_2 and E_1 to form in (e), (f), while vortex D_1 is left behind to pair up with C_2 . Later (D_2 and E_1) will form a pair, followed by (E_2 and F_1) and so on. The resulting 2P mode wake is a set of vortex pairs moving outwards from the wake centerline; the dynamics of the vortex pairs explains the “swinging” of the near wake reported by Öngören and Rockwell [12].

In order to summarize the motion of the vortices at different wavelengths, we look at the vortex positions near the body when it is moving upwards and is crossing the wake centerline in Figure 12. The vortex D_1 (or D) represents the vortex which begins to form in one half cycle, to shed in the next, and to which we paid special attention earlier. At a low wavelength in (a), the acceleration phase of the body motion causes two vortices (D_2 and E_1) to be formed *before* vortex D_1 has reached the rear of the cylinder. The case in (b) represents a “critical” condition in that vortex D_1 (here it is called D) reaches the rear of the body *during* the acceleration phase. This condition we define below as “resonant synchronization”. As the wavelength is increased beyond critical in (c), vortex D_1 is shed much earlier during the half cycle. Then the acceleration phase causes the two vortices (D_2 and E_1) to be formed *after* D_1 is shed.

As the wavelength is increased between (a) and (b), vortex D_1 is able to convect around the cylinder further, until in (b) it arrives at the rear of the cylinder during the acceleration phase, as noted above. Because of this particular timing, the clockwise shear layer does not roll up as a separate entity D_2 as it does in (a), but rather it is rolled up into D_1 (which is shown simply as D here). At this precise wavelength, the resulting formation of a single and more concentrated region of vorticity is interpreted in the present work as the condition of “resonant synchronization”. The “critical curve” shown in the wavelength-amplitude plane in Figure 4 not only gives the

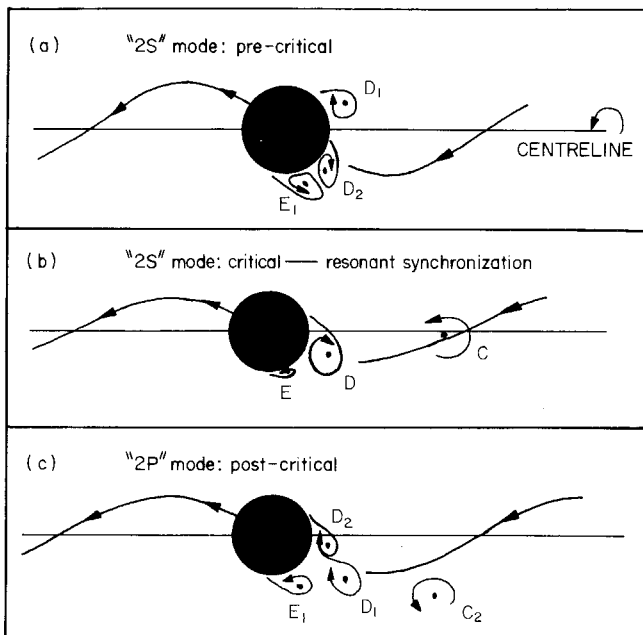


Figure 12. Positions of vortex “D” and other near-wake vortices when the cylinder is travelling upwards, and is just crossing the wake centerline. (a), (b), and (c) are taken from Figures 8(a), 9(a), and 10(e), respectively.

conditions where there is a mode transition of the vortex formation (from a 2S mode to a 2P mode), but it also defines the experimental conditions for this resonant synchronization. It is thus seen that the occurrence of resonant synchronization depends both on the amplitude as well as the wavelength of the body's trajectory. It should also be noted that this curve of resonant synchronization lies close to Bishop and Hassan's curves defining the conditions for a peak in the body forces. It is plausible to assume that their force maxima correspond to the resonant synchronization discussed above, and that the more concentrated distribution of vorticity at this precise wavelength causes the largest body forces; in contrast the dynamics of smaller regions of vorticity (including opposite signs) in the near-wake will induce a smaller rate of change of "impulse" of the shed vorticity distribution, and thereby a smaller force on the body, than is induced by the shedding of more concentrated vortices at resonant synchronization.

To sum up, the acceleration phase of each half cycle of body motion induces two vortices to form, so that four vortices are formed each cycle, except under the particular conditions for resonant synchronization. In the pre-critical case the mutual induction of the vortices causes coalescence of two like-signed vortices each half cycle and the 2S mode will occur, whereas for post-critical the like-signed vortices are convected apart to create the two vortex pairs each cycle that constitute the 2P mode of formation.

The fact that an accelerating body tends to form a fresh pair of vortices has also been found by Honji and Taneda [26], who accelerated a cylinder from one uniform velocity to another. This phenomenon is related to the increasing strength (per unit length) of each of the separating shear layers as the body accelerates which would tend to induce new vortices to roll up near the body, rather like the pair of "starting vortices" that roll up behind a body shortly after an impulsive start. The formation of more than two vortices per cycle (and thus the generation of the P + S and 2P modes) is also apparent in other forced cylinder experiments different from ours, as discussed in Section 3; this can also be attributed to the accelerating components of the relative fluid-body motions in those flows.

Visualization of the 2P mode at the larger amplitude of one diameter is shown clearly in a reference frame fixed with respect to the undisturbed fluid in Figure 13. In (a) and (b), two clockwise vortices are shed as the cylinder travels upwards, followed by the shedding of two anticlockwise vortices in (c), (d) and (e). The vortex pairs then form in the manner described above, convecting outwards as may also be seen from visualization of the downstream wake in Figure 14. Away from the body, the vortices become arranged rather like two parallel vortex streets with fluid moving upstream in two parallel regions, as though caused by two separate bodies upstream.

4.2. EXPLANATION OF THE MODE "JUMP"

Having demonstrated that there is a change from one mode to another as the wavelength is increased, we must now ask why this change should be so abrupt. This question may be addressed by considering a flow that is just precritical and is perturbed by a slight increase of wavelength, so that the flow begins to develop the post-critical mode. In Figure 15, the wake in (a) with a wavelength λ_1 developed vortices A, B, C in the 2S mode. By imposing a new larger wavelength λ_2 , vortex D₁ sheds very slightly earlier, relative to the new half-period, than did C, and allows the roll-up of a small second vortex D₂ in (a) during the remaining part of the cylinder's acceleration phase. The presence of D₂ speeds up the shedding of E₁ in (b), leaving E₂ to grow stronger

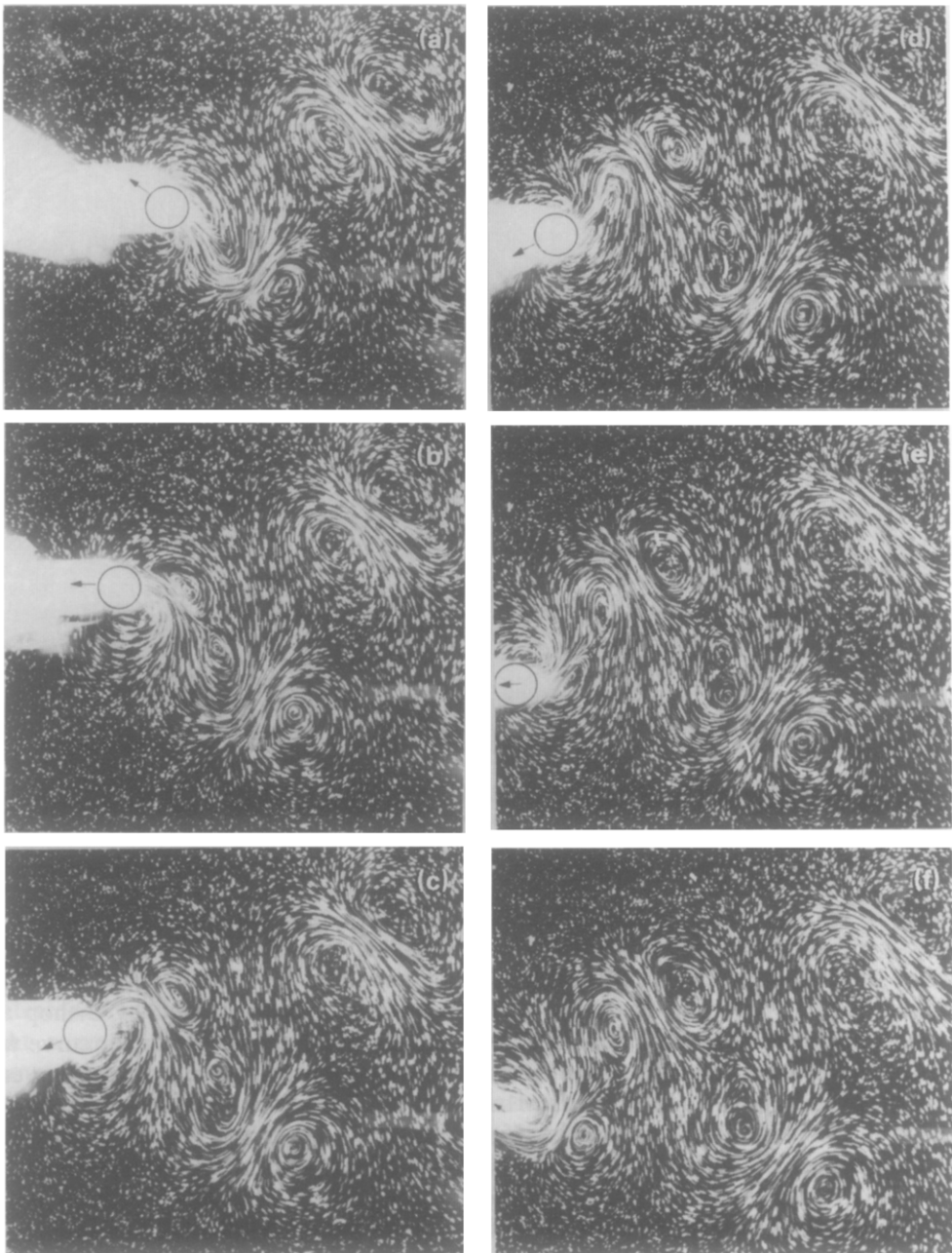


Figure 13. "2P" mode of vortex formation visualized from a reference frame which is fixed with respect to the undisturbed fluid. $\lambda/D = 6.5$, $A/D = 1.0$, $Re = 392$ ($T_e/T_v = 1.33$).

(than D_2). Vortex E_2 speeds up the shedding of F_1 so that it sheds earlier than did E_1 , and so on until a new equilibrium state is reached with vortices shedding close to the start of each new half cycle. The new mode of vortex formation is by now distinctly different from the original mode. It only needs a small disturbance, such as a wavelength increase, to "tip the balance" away from one equilibrium state in favor of another, and thereby cause the abrupt change in formation described as a mode "jump".

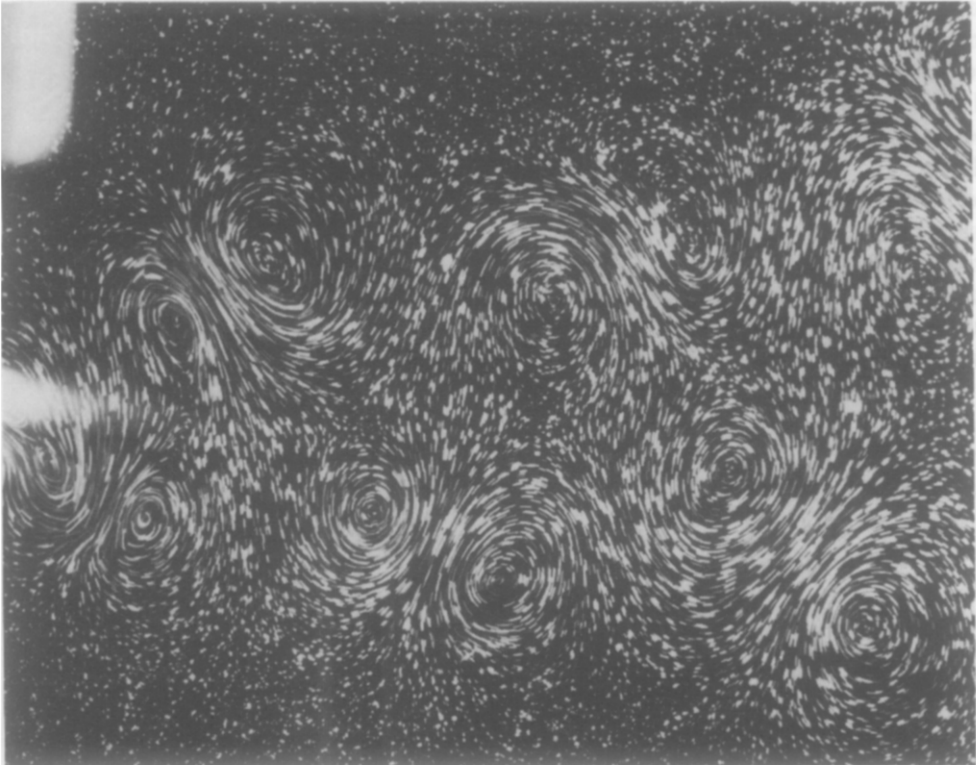


Figure 14. The downstream sequence of vortex pairs from the “2P” mode of vortex shedding of Figure 12. The wake takes on the appearance of two parallel vortex streets.

The mode jump can explain the occurrence of the phase jump and the hysteresis found by Bishop and Hassan. If the vortex shedding occurs earlier in a cycle we may expect an earlier phase of lift, meaning ϕ increases.[†] In Figure 16, a schematic variation of ϕ with λ demonstrates a hysteresis of the kind reported by Bishop and Hassan. The lower curve can be associated with the 2S mode and the upper curve with the 2P mode, where the higher ϕ is consistent with the earlier shedding of vortices each half cycle. It is possible that in a certain range of wavelength λ either of the two equilibrium states or modes can exist. If this is the case, then the chosen mode will be dictated by the history of the flow. The 2P \rightarrow 2S jump will occur for a lower λ than the opposite 2S \rightarrow 2P jump. This then would explain Bishop and Hassan’s hysteresis.

In the next Section, further modes of shedding in the (λ, A) plane are discussed.

5. FURTHER VORTEX SYNCHRONIZATION REGIONS

The fundamental lock-in region discussed above is surrounded by other synchronization regions in the (λ, A) plane. In this section, the P + S, 2P + 2S and coalescence modes are demonstrated, although several features of vortex synchronization are

[†] Define lateral displacement: $y = A \sin \omega t$, and lift coefficient: $C_L \approx C_{L_0} \sin(\omega t + \phi)$, so that an earlier $C_L(t)$ relative to $y(t)$ means an increase in ϕ .

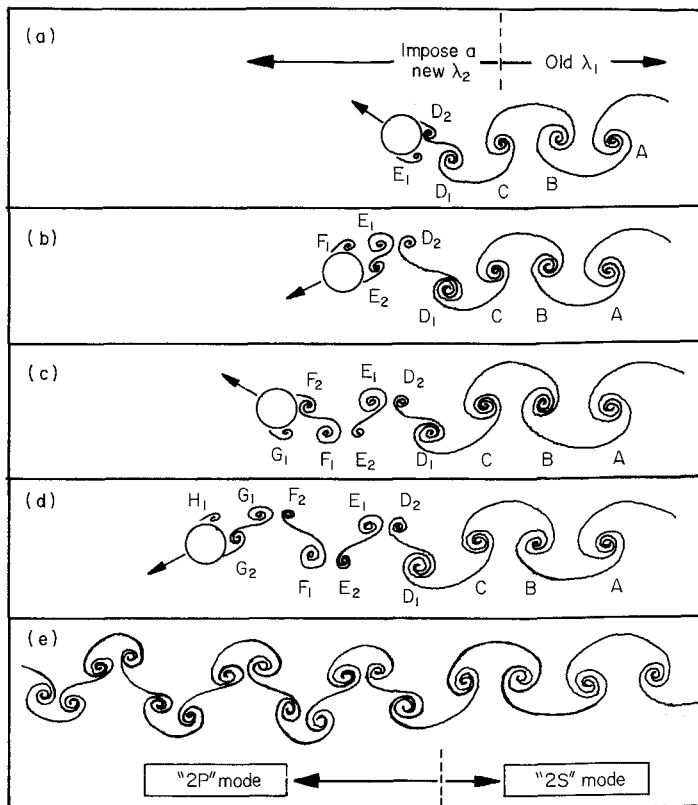


Figure 15. The transition from one equilibrium state of vortex formation (2S) to another equilibrium state (2P) following a small increase in the wavelength of the body trajectory.

omitted here. For example, the downstream wake development, the different types of vortex reorganization, and the scaling of large scale structures due to vortex coalescence will be described elsewhere.

At a small amplitude ($A/D = 0.13$), Öngören and Rockwell [12] reported the recovery of a Karman street when a body is oscillated, over a whole range of frequencies outside the fundamental synchronization region. They found fascinating vortex interactions which caused coalescence to a Karman street, whose size is approximately scaled on the cylinder dimensions. In the present work it was found that for larger amplitudes the wake dimensions did not simply scale on the body size or its oscillation amplitude but could grow to immense proportions, as shown for example in Figure 17(a) for $A/D = 1.0$ and $\lambda/D = 1.5$ ($T_e/T_s = 0.2$). The wake on the right was the result of the coalescence of about 30 smaller vortices into each large vortex, with the typical size of the smaller vortices shown in the small photograph on the left. The wavelength of the large structures is roughly six times the wavelength of a naturally occurring wake, and the large vortices continue to rotate for at least 150 cycles of cylinder oscillation. The scaled body size and trajectory are seen further to the left; at the time of the large photograph the body had reached roughly the position of the arrowhead on the trajectory (relative to the large photograph).

The wakes in Figure 17(b) and (c) are to-scale with the immense wake in (a) and they show the pre-critical 2S mode and the post-critical P + S mode which occurs at this

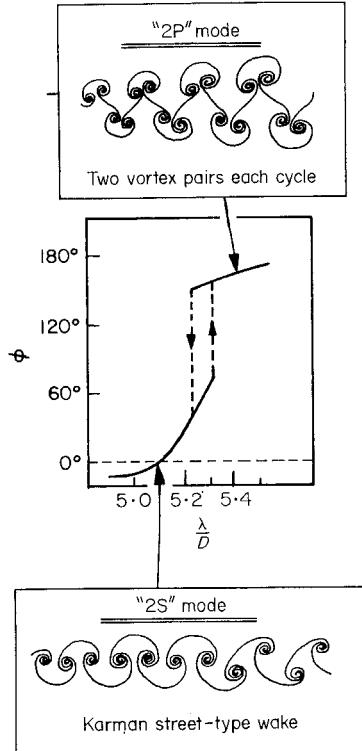


Figure 16. A schematic variation of lift force phase (ϕ) with wavelength (λ), to demonstrate the possibility of hysteresis being caused by an overlap of the regions where the "2S" and "2P" modes occur.

low Re of 275. In (b) there is a sharp increase of lateral vortex spacing at a certain point downstream almost like a "front", but this feature will not be discussed in detail here. The P + S mode in (c) shows the vortex pairs convecting upwards, with the single vortices on the lower side of the wake. The *net* amount of clockwise vorticity within each vortex pair on the upper side must be equal to the negative vorticity in a single vortex on the lower side, and so the clockwise vortex in the pair is stronger than its partner; thus the pairs convect in a curved path away from, then back towards, the wake centerline. To return to Figure 17(a), this wake is also an example of a P + S mode near the cylinder, but with coalescence into the large structure close behind. In this case, the P + S mode causes the enormous structures to be fed with the same amount of clockwise vorticity on the upper side as the amount of anticlockwise vorticity on the lower side of the wake.

The 2P + 2S mode is shown in Figure 18, and can be interpreted as a vortex pair shed at the top and bottom of the body trajectory with single vortices in between. What is interesting about this pattern, and the possible cause of its occurrence, is that it is symmetric, i.e., if a clockwise vortex forms at a certain phase in one half cycle, then the opposite vortex will form at the same phase in the next half cycle. This pattern is drawn schematically in Figure 19(b). When it is found at low amplitudes it represents $T_e \approx 3T_s$ or a $\frac{1}{3}$ -subharmonic, whereas a $\frac{1}{2}$ subharmonic pattern [shown schematically in Figure 19(a)] was not found to occur in the present work. If the coupling between the body motion and the vortex formation is to encourage lock-in during one half cycle

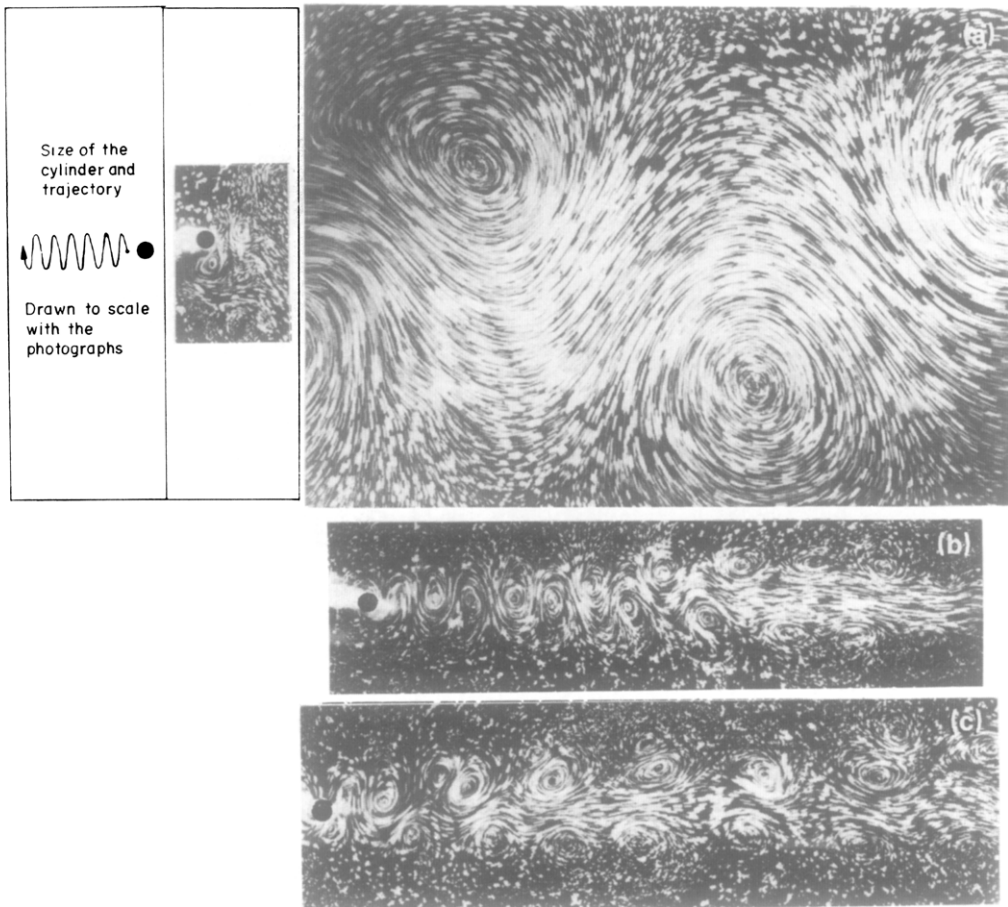


Figure 17. (a) An example of an immense vortex street wake which is caused by the coalescence of a large number of the vortices that are formed in each cycle. $\lambda/D = 1.5$, $A/D = 1.0$, $Re = 60$. ($T_e/T_v = 0.2$). (b) 2S mode for $\lambda/D = 5.5$, $A/D = 0.5$, $Re = 275$. (c) P + S mode for $\lambda/D = 6.0$, $A/D = 0.5$, $Re = 275$. The photographs in (a), (b) and (c) are all to the same scale.

then, because of the symmetry of the 2P + 2S mode, lock-in will be encouraged in the next half cycle. However, the $\frac{1}{2}$ -subharmonic pattern in (a) is not symmetric, and if the body motion would be such as to encourage lock-in during one half cycle, its motion would have an opposite effect on vortex formation in the next half cycle. This may explain the lack of an observed synchronization region in Figure 3 near $\lambda/D \sim 10$, which represents the $\frac{1}{2}$ -subharmonic. The phase of the vortex shedding seemed to change from one cycle to the next one, and lock-on was not observed. Other results of Öngören and Rockwell [12] report a $\frac{1}{2}$ -subharmonic lock-in but not a $\frac{1}{3}$ -subharmonic, whereas in contrast Durgin *et al.* [27] found the $\frac{1}{3}$ -subharmonic but not the $\frac{1}{2}$ -subharmonic, so there are conflicting reports. It seems that the $\frac{1}{2}$ -subharmonic which was noted by Öngören and Rockwell at the low $A/D = 0.13$ does not occur at higher amplitudes, a possible explanation being the symmetry argument above. By extending the argument to other subharmonics we may expect the appearance of $\frac{1}{4}, \frac{1}{5}, \dots$ subharmonic patterns because these are symmetric, and the absence of $\frac{1}{4}, \frac{1}{6}, \dots$ subharmonics as these cannot be symmetric.

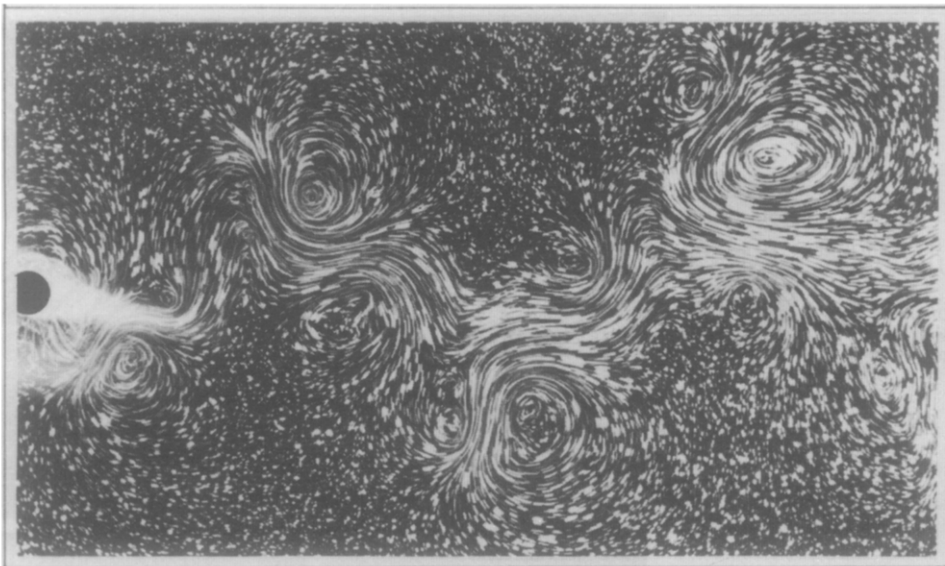


Figure 18. The "2P + 2S" mode of vortex formation represents a $\frac{1}{3}$ -subharmonic pattern, and is symmetric. $\lambda/D = 12.0$, $A/D = 1.15$, $(T_e/T_v = 2.4)$, $Re = 600$.

6. SUMMARY AND CONCLUSIONS

We have explored the existence of vortex synchronization in the wavelength-amplitude plane (which defines the shape of the body trajectory). Several new regions of synchronization occupying this plane have been identified up to amplitudes of five diameters and to wavelengths of 16 diameters. These are summarized below.

There is a regime for small wavelengths where the vortices that are shed in each cycle coalesce in the near wake. When the amplitudes are comparable with the body

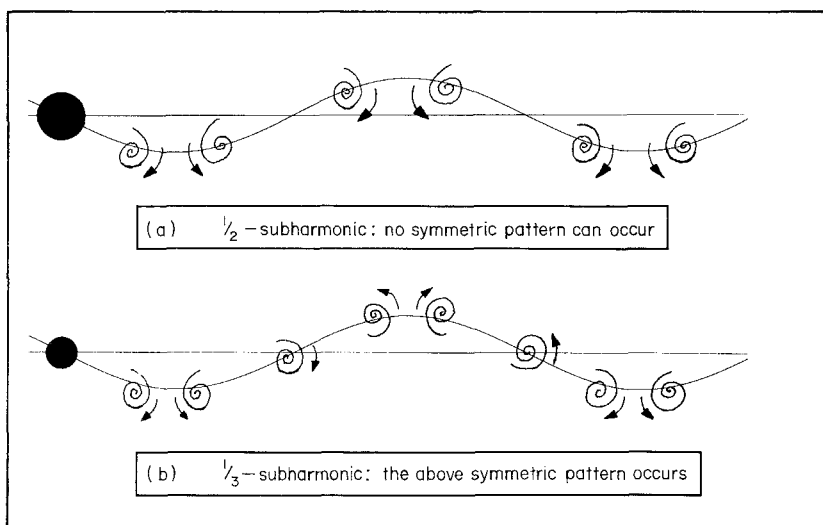


Figure 19. (a) $\frac{1}{2}$ -subharmonic vortex shedding. (b) $\frac{1}{3}$ -subharmonic vortex shedding.

diameter the resulting large-scale vortex street can grow to immense proportions. At larger amplitudes, different vortex patterns are synchronized, each within a certain range of amplitude, and these are similar to those patterns found previously for an oscillating body without a mean flow. They involve the formation of vortex pairs which can convect away from the body, forming jets as well as wakes. Despite the symmetry of the body motion, these patterns can be distinctly asymmetric.

A further synchronized vortex wake, which has been observed here, involves the generation of six vortices per cycle. Where the pattern occurs for low amplitudes and large wavelengths, it represents a $\frac{1}{3}$ -subharmonic lock-in; i.e., the excitation frequency is around one third of the natural shedding frequency. It is argued that the appearance of a $\frac{1}{3}$ -subharmonic pattern and the absence of one at the $\frac{1}{2}$ -subharmonic is due to symmetry requirements of the wake patterns between each half cycle of body motion.

The well-known lock-in occurs when the trajectory wavelength is comparable with the distance a non-oscillating cylinder travels through the fluid in one cycle of shedding. In this fundamental lock-in region, the acceleration phase of the body motion at the start of each half cycle has the effect of rolling-up both of the separating shear layers into a fresh pair of vortices. The continuously accelerating/decelerating body thereby sheds four regions of vorticity each cycle, rather than simply two Karman-type vortices as was previously assumed. Below a critical trajectory wavelength, each half cycle sees the coalescence of two like-signed vortices, so that two regions of opposite vorticity are fed into the wake per cycle. This mode of formation creates a Karman street-type wake (or 2S mode). If, however, the wavelength exceeds a critical value, each of the two like-signed vortices pairs up with an opposite-signed vortex. The resulting wake comprises a system of vortex pairs convecting away from the wake centerline (in the 2P mode). What is significant about the transition from the first mode to the second mode is that it coincides with, and is a plausible explanation of, the sharp change in the character of the body forces that was found by Bishop and Hassan [3] in 1964. Any sharp change in the phase of the lift force (with respect to the body motion) must be associated with an abrupt change in the dynamics of the wake vortices. The fact that beyond a critical wavelength the phase changes suddenly or "jumps" is caused by the inception of vortex pairing each half cycle, which causes a sharp change in the timing of the vortex shedding. Over a small range of wavelengths either of the two modes described above may exist, with the chosen mode depending on the flow history. This would explain the hysteresis in Bishop and Hassan's force measurements. The formation of more than two vortices per cycle discussed above (and thus the generation of the 2P or P + S modes) is also apparent in a number of other forced cylinder experiments different from ours, and can also be attributed to the accelerating components of the relative body-fluid motions in those flows.

When the wavelength of the trajectory is increased up to the critical value discussed above, the four regions of vorticity are then not formed. At this precise wavelength, the timing is such that one of the shear layers that separates during the acceleration, instead of rolling up as a separate entity, is rolled into one of the vortices which began its life in the previous half cycle. The result is that only two vortices are formed each cycle, and the wake vorticity is more concentrated. We interpret this case as the condition of "resonant synchronization" within the lock-in region. A critical curve in the amplitude-wavelength plane, which defines where the resonant synchronization (and also the mode transition) occurs, is approximately coincident with the curve where a peak in body forces was observed by Bishop and Hassan. It seems apparent that this peak is caused by the resonant synchronization described above, and that the largest forces are induced by the shedding of more concentrated regions of vorticity;

however, some further work will have to be done to confirm this. For this purpose, we are planning to extend the present experiments to include measurements of force.

It is possible that further "resonances" between the body motion and the wake formation (and thereby further resonances in the cylinder forces) may exist in other parts of the wavelength-amplitude plane. It is intended to investigate such resonances, as well as to study over what range of Reynolds numbers the present conclusions will apply.

ACKNOWLEDGEMENTS

This research was supported by the Office of Naval Research under contract number N00014-84-C-0618. The authors are indebted to R. Paniagua for the skillful construction of the X-Y tow tank and test bodies.

REFERENCES

1. P. W. BEARMAN 1984 Vortex shedding from oscillating bluff bodies. *Annual Review of Fluid Mechanics* **16**, 195–222.
2. T. SARPKAYA 1979 Vortex induced oscillations. *Journal of Applied Mechanics* **46**, 241–258.
3. R. E. D. BISHOP and A. Y. HASSAN 1964 The lift and drag forces on a circular cylinder oscillating in a flowing fluid. *Proceedings of the Royal Society (London), Series A* **277**, 51–75.
4. C. C. FENG 1968 The measurement of vortex-induced effects in flow past stationary and oscillating circular and D-section cylinders. MSc thesis, University of British Columbia, Vancouver, B.C., Canada.
5. R. T. HARTLEN, W. D. BAINES and I. G. CURRIE 1968 Vortex excited oscillations of a circular cylinder. University of Toronto, Mechanical Engineering Department, Report UTME-TP6809, Toronto, Ontario, Canada.
6. E. BERGER 1984 Zwei fundamentale Aspekte wirblerregter Schwingungen. Report B.E. 343/12, Technische Universität, Berlin.
7. M. M. ZDRAVKOVICH 1982 Modification of vortex shedding in the synchronization range. *ASME Journal of Fluids Engineering*. **104**, 513–517.
8. J. P. DEN HARTOG 1934 The vibration problem in engineering. *Proceedings of 4th International Congress in Applied Mechanics*, Cambridge, England, pp. 34–53.
9. A. MEIER-WINDHORST 1939 Flatterschwingungen von Zylindern in gleichmässigen Flüssigkeitsstrom. *Mitteilungen des Hydraulischen Instituts der Technischen Hochschule, München, Heft* **9**, 3–39.
10. F. ANGRILLI, G. DI SILVIO, and A. ZANARDO 1974 Hydroelasticity study of a circular cylinder in a water stream. In *Flow-Induced Structural Vibrations* (ed. E. Naudascher), pp. 504–512. Berlin: Springer-Verlag.
11. O. M. GRIFFIN and S. E. RAMBERG 1974 The vortex street wakes of vibrating cylinders. *Journal of Fluid Mechanics* **66**, 553–576.
12. A. ÖNGÖREN and D. ROCKWELL 1987 Flow structure form an oscillating cylinder. Part 1: Mechanisms of phase shift and recovery in the rear wake. Submitted to *Journal of Fluid Mechanics*.
13. M. J. Lighthill 1986 Fundamentals concerning wave-loading in offshore structures. *Journal of Fluid Mechanics* **173**, 667–681.
14. P. K. STANSBY 1976 Base pressure of oscillating circular cylinders. *Journal of Engineering Mechanics Division of ASCE*. **EM4**, 591–600.
15. C. H. K. WILLIAMSON 1985 Sinusoidal flow relative to circular cylinders. *Journal of Fluid Mechanics* **155**, 141–174.
16. C. H. K. WILLIAMSON and A. ROSHKO 1986 Studies of vortex interactions. In *Proceedings of the Symposium for the Fortieth Anniversary of the Office of Naval Research*, Washington, D.C., U.S.A.
17. C. H. K. WILLIAMSON and A. ROSHKO 1986 Vortex dynamics in the wake of an oscillating cylinder. *Bulletin of the American Physical Society*. **31**, 1690.
18. P. W. BEARMAN, J. M. R. GRAHAM, P. NAYLOR, and E. D. OBASAJU 1981 The role of

- vortices in oscillatory flow about bluff cylinders. In *International Symposium on Hydrodynamics and Ocean Engineering*, Trondheim, Norway, pp. 621–626.
- 19. G. H. KOOPMANN 1967 The vortex wakes of vibrating cylinders at low Reynolds numbers. *Journal of Fluid Mechanics* **51**, 31–48.
 - 20. M. M. KOOCHESFAHANI 1987 Vortical patterns in the wake of an oscillating airfoil. AIAA Paper 87-0111.
 - 21. O. M. GRIFFIN and S. E. RAMBERG 1976 Vortex shedding from a cylinder vibrating in-line with an incident uniform flow. *Journal of Fluid Mechanics* **75**, 257–271.
 - 22. A. ÖNGÖREN and D. ROCKWELL 1987 Flow structure from an oscillating cylinder. Part II: Mode competition in the near wake. Submitted to *Journal of Fluid Mechanics*.
 - 23. Y. COUDER and C. BASDEVANT 1986 Experimental and numerical study of vortex couples in two-dimensional flows. *Journal of Fluid Mechanics* **173**, 225–251.
 - 24. E. DETEMPLE 1987 Zur Phänomenologie Karmanscher Wirbelstrassen in durch Schall überlagerter Strömung. *Mitteilungen aus dem Max-Planck-Institut für Strömungsforschung*, Göttingen, Nr. 84.
 - 25. H. HONJI and S. TANEDA 1968 Vortex wakes of oscillating circular cylinders. *Report of the Research Institute of Applied Mechanics*. (Kyushu University, Japan) **16**, 211–222.
 - 26. H. HONJI and S. TANEDA 1969 Time dependent flow around a circular cylinder accelerated uniformly from one speed to another. *Report of the Research Institute of Applied Mechanics* (Kyushu University, Japan) **17**, 187–193.
 - 27. W. W. DURGIN, P. A. MARCH and P. J. LEFEBVRE 1980 Lower mode response of circular cylinders in cross-flow. *ASME Journal of Fluids Engineering* **102**, 183–190.